Research Journal of Applied Sciences, Engineering and Technology15(3): 118-123, 2018
DOI:10.19026/rjaset.15.5836
ISSN:2040-7459; e-ISSN: 2040-7467

Submitted: November 3, 2017 Accepted: January 10, 2018 Published: March 15, 2018

Research Article

Effect of Laser Welding Parameters on Weld Bead Geometry

Reuven Katz,Anton Zak and AmnonShirizly
Department of Mechanical Engineering,TechnionTechnion City, Haifa, 3200003, Israel

Abstract: The aim of the study was the development of models that describe Laser beam welding process of maraging steel 250 sheets, based on measured experimental data. Maraging steel 250 is widely used in applications that require high strength steel. For example, in aerospace industry, to produce engine components, or in sports industry, to produce bicycle frames or golf club heads. In order to achieve a reliable and repeatable welding process, we investigated the influence of welding parameters on the welded process responses, i.e., weld penetration depth and bead width. Two modeling techniques for predicting weld bead geometry were developed and tested. One method is the Multiple Regression Analysis (MRA) which is widely used for modeling welding processes and the other is Artificial Intelligence (AI) technique, which is rarely applied for modeling welding processes. The MRA method uses polynomials to express the relations between bead geometry and welding parameters, while the AI method is more flexible and presents in the model terms with physical meaning. Both MRA and AI models present similar statistical quality of fit between the predicted values of bead geometry and the actual experimentally measured data.

Keywords: AI model, laser beam welding, MRA

INTRODUCTION

Laser Beam Welding (LBW) is widely used in various industrial applications for high quality joining of mechanical elements (Schlüter, 2007). Due to the high power density of the laser beam, LBW is characterized by a narrow weld width and high penetration, a narrow heat-affected zone and minimal distortion of the workpiece. The selected combination of input parameters determines the geometry of the laser weld bead and its quality. The main input parameters that control process quality are laser power, welding speed, focal depth and shielding gas (Huang *et al*., 1991).

In the current investigation, two methods are used to model weld bead formation: Multiple Regression Analysis (MRA); and Artificial Intelligence(AI), which uses evolutionary search of experimental data to determine mathematical equations. Wu and Ume (2012) applied stepwise regression analysis to predict penetration depth of butt welds in thin plates. Lee and Um (2000) modeled a gas metal arc welding process by using the multiple regression analysis and neural network. Benyounis*et al*. (2005) applied linear regression to model welding parameters to predict four responses: heat input, weld width, weld penetration and the geometry of the heat affected zone. Eureqa is an AI-powered modeling engine that uses evolutionary search to determine mathematical equations that describe sets of data in their simplest form (Schmidt and Lipson, 2009). The software automatically builds analytical models and allows experts to evaluate their physical meaning (Popraweet*et al*., 2010). Devrient*et al*. (2013) utilized Eureqa to fit welding parameters in a laser transmission welding of thermoplastics with dual clamping devices; however, they did not use it for weld modeling purposes.

Additional method proposed by several researchers for modeling weld geometry in various welding processes, is Artificial Neural Network (ANN) (Ghosh *et al*., 2007; Kim *et al*., 2003). The model received by ANN method is typically a complicated mathematical expression that does not present any physical insight. Towsyfyan*et al*. (2013) showed that in modeling Submerged Arc Welding process the ANN method presented result that were in good agreement with the MRA method.

In our study, the experimental plan was developed using a D-optimal design method. Twenty-three welding experiments and an additional three validation experiments were performed. Seven laser input parameters were measured in the experiment: laser power, welding speed, focal depth, focal diameter, shield gas nozzle distance from the workpiece, shield

Corresponding Author: Reuven Katz, Department of Mechanical Engineering, Technion, Technion City, Haifa, 3200003, Israel

Table 1: Welding parameters and their levels

Parameter	Code	Unit	L1	L2	L3
Laser power	LP	Watt	1000	2000	3000
Welding speed	S	m/min	2	3	5
Focal depth	F	Mm	0	1.5	3
Shield gas tilt	TET	Degrees	20	-	30
Focal diameter	D	Mm	0.378	0.513	0.693
Work piece cleanness	CM	-	None	Acetone	Polish+ Acetone
Shield gas distance	N	Mm	6	10	15

gas tilt angle and the cleanness level of the workpiece's surface.

MATERIALS AND METHODS

Materials: Maraging steel 250 with chemical nominal composition in weight percent of 18.46% Ni, 8.3% Co, 4.7% Mo, 0.45% Ti, 0.1% Al, 0.01% C and Fe balance, was used as workpiece material. The size of each welded plate was 200×100 mm and its thickness 4.5 mm.

Experiment plan and execution: The experiment was planned using D-optimal design (Heredia-Langner*et al*., 2003). The D-optimality criterion seeks to maximize the determinant of the information matrix$X'X$ of a specific experiment design. The independent input variables and their values are presented in Table1.

Second order polynomials were fitted to the experimental data to obtain the regression equations. The general expression of the second order polynomials (Montgomery, 2001) is presented in Eq. (1):

$$Y = b_0 + \sum b_i X_i + \sum b_{ii} X^2_{ii} + \sum b_{ij} X_i X_j \quad (1)$$

A multivariate regression method was applied to fit this explicit expression to the experimental data to identify the required b_{ij} coefficients (Montgomery, 2001).

The experiments were carried out using 4-kW Ytterbium Fiber Laser, model YLS-4000-CT-WW from IPG Laser GmbH. Pure argon was used as the shielding gas. The experimental setup is presented in Fig. 1. The experiment was performed according to the design table in random order to avoid systematic errors. Additional information about the experiment is available in (Katz *et al*., 2017).

Two transverse specimens were cut from each weld. A standard metallographic cross-section was made for each transverse specimen. The bead profile geometry, i.e., penetration and width, was measured using an optical microscope. An integrated software package that amplifies the image ×100 allows measurement of weld bead dimensions within 0.001 mm accuracy. The average of two measured profile parameters was logged for each experiment. Two examples of bead geometry cross-sections are shown in Fig. 2. On the left is a typical cross-section for a low laser power and low welding speed weld. On the right is a typical cross-section for a high laser power and

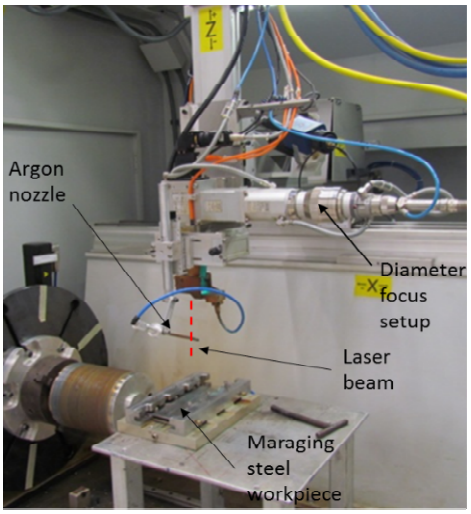

Fig. 1: Experimental setup

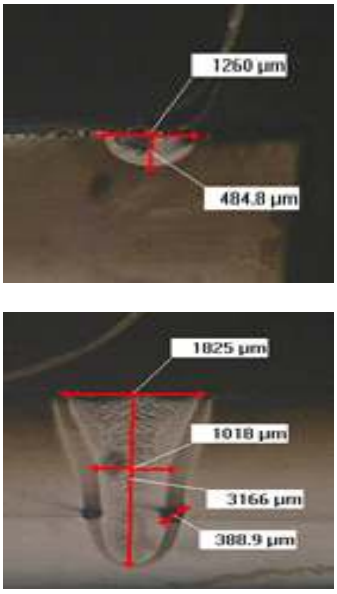

Fig. 2: Measured bead geometry (on the left: low power & low welding speed weld; on the right: high power and high welding speed weld)

high welding speed weld, the images were analyzed using the method in (Steiner and Katz, 2007).

During the welding process, heat input to the workpiece is produced by the laser beam and it depends on welding speed. The value of *heat input* can be calculated for each experiment, since*heat input* =

Table 2: Experimental design matrix and experimental responses

Welding parameters							Measured responses	
LP (watt)	S (m/min)	F (mm)	TET (deg)	D (mm)	CM	N (mm)	Penetration depth	Weld width
2000	3	1.5	20	0.378	L1	10	2.565	2.513
2000	2	0	30	0.513	L3	15	2.64	2.23
1000	2	0	30	0.378	L1	6	1.97	1.961
1000	5	0	30	0.693	L3	15	0.633	1.16
2000	5	0	30	0.693	L2	6	1.209	2.08
1000	2	1.5	30	0.693	L2	15	1.127	1.75
1000	5	0	20	0.513	L2	10	0.97	1.28
1000	2	3	20	0.693	L1	15	1.071	1.924
3000	3	3	30	0.513	L2	6	3.34	2.8
3000	2	3	30	0.378	L1	15	4.182	3.78
3000	5	3	30	0.378	L3	10	2.78	1.96
1000	5	3	30	0.693	L1	6	0.541	1.275
1000	2	3	30	0.378	L3	10	1.804	1.813
1000	5	3	20	0.378	L2	15	0.8	1.22
3000	2	1.5	30	0.693	L1	6	4.074	3.637
1000	2	0	20	0.693	L3	6	1.13	1.73
3000	2	1.5	20	0.378	L3	6	3.93	3.02
3000	5	0	20	0.513	L1	6	2.867	2.053
2000	2	3	20	0.513	L2	6	3.068	3.084
3000	5	1.5	30	0.513	L2	15	2.65	2.043
3000	3	3	20	0.693	L3	15	3.026	2.624
3000	2	0	20	0.693	L2	10	4.2	3.46
1000	5	1.5	20	0.378	L3	6	1.127	1.241

η*(LP/S), where η, energy transfer efficiency, is in the range of 0.7-0.8 (Fuerschbach, 1996) and both LP and S are known input parameters.

The experiments were performed in a random order following the optimal design matrix shown in Table 2. Table 2 also includes the measured responses obtained from the 23 welding experiments: weld penetration depth and weld bead width. The responses of weld bead geometry were measured using transverse sectioned specimens and an optical microscope.

Methods for modeling weld bead geometry: Two methods were used to model bead geometry, i.e., depth of penetration and weld bead width: multiple regression analysis and the AI technique.

Multiple Regression Analysis (MRA) method: The modified quadratic model in Eq. 2 was used to fit the experimental responses listed in Table 2. We tested the significance of the regression models, the significance of individual model coefficients and lack of fit utilizing ANOVA with JMP 13 statistical software. The multivariate regression method designates which are the significant parameters in the model.

Penetration depth: Fig. 3 presents the fit between the predicted and actual values. The predicted values were calculated using the penetration depth model in Eq. (2) and the actual values represent the 23 experimental results in Table 2. R^2 = 0.95, RMSE = 0.276 and p-valu<0.0001 represent a very good fit between the predicted and actual responses:

$$PenetrationDepth[mm] = 2.0089 + 0.0011LP - 0.3510S - 1.4471D - 1.0289 \cdot 10^{-4}(LP - 1956.5217)(S - 3.3043) \quad (2)$$

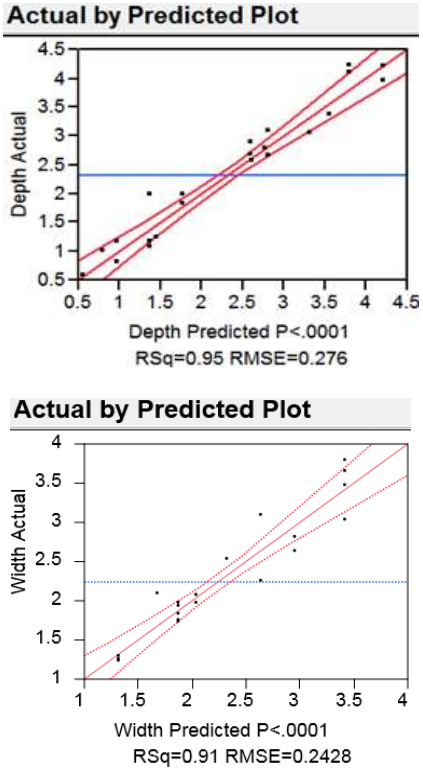

Fig. 3: Predicted vs. actual fit: penetration depth (left), weld bead width (right)

Equation 2 shows that as increasing laser power increases heat input to the workpiece, more metal volume is molten, therefore increasing penetration depth. Increasing welding speed (S) decreases heat input and as result, decreases weld penetration.

Decreasing the focal diameter (D) increases the laser power density, which means the heat will localize in a small metal area and therefore penetration depth increases. To achieve maximum penetration depth, one should increase LPand decrease S and D. Benyounis*et al*. (2005) presented an empirical relation of weld penetration that depends on the parameters LP, S and F.

Weld bead width: Fig. 3 (on the right) shows the fit between the predicted and actual values of weld bead width. The predicted values were calculated using the weld zone width model according to Eq. (3) and the actual measured values are from Table 3. R^2 = 0.91, RMSE = 0.243 and p-value<0.0001 represent a good fit between predicted and actual responses. The empirical model for weld bead width is presented in Eq. (3):

$$WeldBeadWidth[mm] = 2.0485 + 6.0663 \cdot 10^{-4} LP - 0.3176S - 1.3335 \cdot 10^{-4} (LP - 1956.5217)(S - 3.3043) \quad (3)$$

Equation (3) shows that increasing laser power LP increases the weld zone width. Conversely, increasing the welding speed decreases weld zone width.

Artificial intelligence method: Eureqa is an Artificial Intelligence (AI) powered modeling engine. The software uses evolutionary algorithms to determine mathematical equations that describe sets of data in their simplest form. An evolutionary algorithm uses mechanisms inspired by biological evolution. Using the collected experimental data, we decided to find a model for bead geometry, i.e., penetration depth and weld bead width.

Weld penetration depth: Based on our experimental results shown in Table 2, the best equation that represents penetration depth is shown in Eq. (4):

$$PenetrationDepth[mm] = 5.32 \cdot 10^{-4} LP + 0.0017(LP / S) \quad (4)$$

Here we received the following calculated values: R^2 = 0.947, RMSE = 0.275, Correlation coefficient = 0.973 and Mean squared error = 0.0759. These results represent very good fit between predicted and actual values. Eq. (4) is simpler than Eq. (2), which also describes penetration depth and was obtained by multiple regression analysis. Eq. (4) does not include the parameter D and interestingly it includes the term LP/S, which is directly proportional to the expression of heat input.The structure of Eq. (4) is similar to the empirically determinedEq. (1), presented by Norris *et al*. (2011).

Weld bead width: Based on our experimental data shown in Table 2, the best equation that represents weld bead zone is that shown in Eq. (5):

$$WeldBeadWidth[mm] = 1.01 + 0.00167(LP / S) \quad (5)$$

The calculated values of R^2 = 0.916, RMSE = 0.223, Correlation coefficient = 0.957 and Mean squared error = 0.0498 represent good fit between the predicted and actual values. As observed in Eq. (5), weld bead width is dependent on a constant value and a value proportional heat input (LP/S). Again, it is a simpler expression than Eq. (3), which was obtained by the MRA method and may be physically interpreted. The higher the heat input (LP/S), the more material is molten and both the depth penetration and weld bead width increase.

RESULTS AND DISCUSSION

Comparison of MRA and AI methods: Table 3 compares the statistical quality of fit between the predicted values proposed by each of the two models and the actual values measured in the 23 experiments. The coefficient of determination (R^2) as well as the Root Mean Squared Error (RMSE) of the MRA and AI methods are almost identical. The AI modeling engine proposed a mathematical model that contains simple terms representing heat input during welding. The MRA model comprises of polynomial terms and is slightly more complicated; however, it captures the correct influence of the parameters LP and S and D on bead geometry.

Experimental verification of the models: At the end of the 23 experiments required to find the model parameters, we performed an additional 3 experiments to verify the fit between the model and the actual measured values. Welding parameters as well as the measured responses are presented in Table 4. The relative error, calculated by (predicted value-measured value)/measured value, is also presented in Table 4 for each method. All relative errors are under 10% and represent good fit between the predicted values and the measured experimental results.

Discussion: The study presents a method for selecting optimal number of welding experiments needed to create a database that allows developing a welding model. The aim of this welding model is to generate relationship between selected welding parameters and the required responses. By applying the model, one may predict bead geometry for a specific set of welding parameters. Multiple Regression Analysis is the leading method for modeling weld bead geometry (Benyounis*et al*., 2005). The MRA method uses polynomials to describe the relations between welding parameters and the responses. MRA show good fit with the experimental data and can be used to predict welding parameters for some specified geometry requirements. The second method that was applied in the study is artificial intelligence. The authors could not find references that used artificial intelligence for modeling

Table 3: Comparison of the two methods

	MRA		AI (Eureqa)	
Measured responses	R^2	RMSE	R^2	RMSE
Penetration depth	0.95	0.276	0.947	0.275
Weld bead width	0.91	0.243	0.916	0.223

Table 4: Measured vs. predicted responses and relative errors

Exp #	LP (Watt)	S (m/min)	D (mm)	Parameters values	PD (mm) (%)	Error (PD)	WW (mm)	Error (WW) (%)
1	3000	3	0.513	Measured	3.424		2.859	
				Pred. (MRA)	3.561	4.00	2.956	3.39
				Pred. (AI)	3.296	-3.74	2.680	-6.26
2	1000	2	0.378	Measured	1.270		1.890	
				Pred. (MRA)	1.380	8.66	1.870	-1.06
				Pred. (AI)	1.382	8.82	1.845	-2.38
3	3000	2	0,378	Measured	4.118		3.650	
				Pred. (MRA)	3.808	-7.53	3.413	-6.49
				Pred. (AI)	4.146	0.68	3.515	-3.70

weld bead geometry. AI method allows flexibility in selecting mathematical expressions to be used in the model. We found that the AI model comprises terms with a physical meaning such as the *heat input term* (*LP/S*).It presents natural relations between welding parameters and the responses, i.e., the larger is the heat input that the laser transfers to the joint during the welding process, the deeper is welding penetration and wider is the weld bead. The AI weld penetration model, described in Eq. (4) has a similar structure as the empirical model proposed by Norris *et al*. (2011). The models developed using both methods showed almost similar quality and were verified experimentally. The proposed methods for building welding models may be generalized and used to prepare practical tools for improving welding processes for various welding configurations and for different materials.

CONCLUSION

- The study presents a model based on multiple regression analysis that is capable of predicting weld bead geometry. The model was verified experimentally to show good fit with the predicted responses.
- An artificial intelligence method was successfully used to develop a mathematical model based on a similar experimental data for predicting weld bead geometry. The AI model includes simpler expressions with a physical meaning.
- Both MRA and AI models have similar statistical quality of fit between the predicted values and the actual experimental data.

ACKNOWLEDGMENT

We would like to acknowledge Benny Tavlovich, ElieLouzon and AmiramLeitner for their contribution to this study.

CONFLICT OF INTEREST

The authors state that there is no financial or other conflict of interest that influenced the development of the manuscript.

REFERENCES

Benyounis, K.Y., A.G. Olabi and M.S.J. Hashmi, 2005. Effect of laser welding parameters on the heat input and weld-bead profile. J. Mater Process Technol., 164-165: 978-985.

Devrient, M., B. Knoll and R. Geiger, 2013. Laser transmission welding of thermoplastics with dual clamping devices. Phys. Procedia, 41:70-80.

Fuerschbach, P.W., 1996. Measurement and prediction of energy transfer efficiency in laser beam welding. Weld. J., 75: 24s-34s.

Heredia-Langner, A., W.M. Carlyle, D.C.Montogomery, C.M. Borrorand G.C. Runger, 2003. Genetic algorithms for the construction of D-optimal designs. J. Qual. Technol., 35: 28-46.

Huang, Q., J. Hagstroem, H. Skoog and H. Kullberg, 1991. Effect of laser parameter variation on sheet metal welding. Int. J. Joining Mater, 3(3):79-88.

Ghosh, A., S. Chattopadhyaya and P.K. Sarkar, 2007. Effects of input parameters on weld bead geometry of saw process. Proceeding of the International Conference on Mechanical Engineering (ICME 2007), Dec. 29-31, 2007.

Katz, R., A. Zak, A. Shiirizly, A. Leitner and E. Louzon, 2017. Method for producing porosity-free joints in laser beam welding of Maraging steel 250. Int. J. Adv. Manuf. Tech., 94(5-8): 2763-2771.

Kim, I.S., J.S. Son, I.G. Kim, J.Y. Kim and O.S. Kim, 2003. A study on relationship between process variables and bead penetration for robotic CO2 arc welding. J. Mater. Process. Tech., 136(1-3):139-145.

Lee, J. and K. Um, 2000. A comparison in a back-bead prediction of gas metal arc welding using multiple regression analysis and artificial neural network. Opt. Laser. Eng., 34(3):149-158.

Montgomery, D.C., 2001. Design and Analysis of Experiments. 5th Edn., John Wiley and Sons, New York, pp: 436-440.

Norris, J.T., C.V. Robino, D.A. Hirschfeld and M.J. Perricone, 2011. Effects of laser parameters on porosity formation: Investigating millimeter scale continuous wave Nd: YAG laser welds. Weld. J., 90(10): 198s-203s.

Popraweet, R., W. Schulze and R. Schmitt, 2010.Hydrodynamics of material removal by melt expulsion: Perspectives of laser cutting and drilling. Phys. Procedia, 5: 1-18.

Schlüter, H., 2007.Laser beam welding: Benefits, strate gies, and applications. Weld. J., 86(5): 37-39.

Schmidt, M. and H. Lipson, 2009. Distilling free-form natural laws from experimental data. Science, 324(5923): 81-85.

Steiner, D. and R. Katz, 2007. Measurement techniques for the inspection of porosity flaws on machined surfaces. J. Comput. Inf. Sci. Eng., 7(1): 85-94.http://computingengineering.asmedigitalcollecti on.asme.org/article.aspx?articleid=1400729

Towsyfyan, H., G. Davoudi, B.H. Dehkordy and A. Kariminasab, 2013. Comparing the regression analysis and artificial neural network in modeling the Submerged Arc Welding (SAW) process. Res. J. Appl. Sci. Eng. Technol., 5(9): 2701-2706.

Wu, T.Y. and C.I. Ume, 2012. Prediction and experimental validation of penetration depth of butt welds in thin plates using superimposed laser sources. NDT&E Int., 50: 10-19.